A Graphical Tool and Methods for Assessing Margin Definition From Daily Image Deformations

Aditya P Apte, R Al-Lozi, G Pereira, M Johnson, D Mansur, I El Naqa*
Department of Radiation Oncology, School of Medicine, Washington University in Saint Louis, MO, 63110, USA

ABSTRACT

Estimating the proper margins for the planning target volume (PTV) could be a challenging task in cases where the organ undergoes significant changes during the course of radiotherapy treatment. Developments in image-guidance and the presence of onboard imaging technologies facilitate the process of correcting setup errors. However, estimation of errors due to organ motions remain an open question due to the lack of proper software tools to accompany these imaging technological advances. Therefore, we have developed a new tool for visualization and quantification of deformations from daily images. The tool allows for estimation of tumor coverage and normal tissue exposure as a function of selected margin (isotropic or anisotropic). Moreover, the software allows estimation of the optimal margin based on the probability of an organ being present at a particular location. Methods based on swarm intelligence, specifically Ant Colony Optimization (ACO) are used to provide an efficient estimate of the optimal margin extent in each direction. ACO can provide global optimal solutions in highly nonlinear problems such as margin estimation. The proposed method is demonstrated using cases from gastric lymphoma with daily TomoTherapy megavoltage CT (MVCT) contours. Preliminary results using the Dice similarity index are promising and it is expected that the proposed tool will be very helpful and have significant impact for guiding future margin definition protocols.

Keywords: margin definition, organ motion, daily imaging, graphical tool, ant colony optimization
Disclosure: The authors declare no conflicts of interest.

1. INTRODUCTION

Geometrical accuracy is an important requisite for conformal radiotherapy in order to ensure coverage of the tumor while avoiding critical organs at risk. This is particularly the case with the latest advances in intensity modulated radiotherapy treatment planning (Webb, 2005). There are several sources of error that can cause geometrical uncertainty such as (van Herk, 2004): (1) limited resolution of CT images; (2) contouring variations; (3) setup errors, and (4) organ motion. In particular, it is noticed that the estimation of the proper margins for the planning target volume (PTV) could be a challenging task in cases where the organ undergoes significant changes during the course of fractionated radiotherapy treatment resulting in both systematic and random errors. Therefore, we have developed a new tool for visualization and quantification of deformations from daily images. Such daily images are becoming more available in the treatment room, thanks to recent advances in onboard imaging technologies such as megavoltage CT (MVCT) with TomoTherapy (TomoTherapy, Inc., Madison, WI) and conebeam CT with the Varian Trilogy (Varian Medical Systems, Inc., Palo Alto, CA) and other manufacturers as well.

Our developed tool utilizes daily imaging information for estimation of tumor coverage and normal tissue exposure as a function of selected margin (isotropically or anisotropically). This information would be very helpful and have significant impact for guiding future margin definition protocols. As a demonstrative example we will consider the case of target definition for stomach lymphoma, where the stomach changes significantly from day to day. A common practice is to add a constant 1-2 cm margin isotropically around the tumor volume based on the planning CT scan. This might lead to some portions of the stomach being under-dosed or surrounding normal structures over-dosed. The purpose of this work is to develop a tool that utilizes information from daily MVCT images to aid localization of these deformations and guide estimations of proper margins.

*elnaqa@wustl.edu; phone +1 314 362 0129; fax +1 314 362 8521; radonc.wustl.edu

doi: 10.5166/jroi-2-1-7
ISSN: 1663-618X, J Radiat Oncol Inform 2010; 2:1:9-19

2. ORGAN MOTION PROBABILITY

The margin estimation process for selected organ motion probability builds on the existing functionality in the open-source tool for data de-archiving and analysis CERR (A Computational Environment for Radiotherapy Research)(Deasy, Blanco and Clark, 2003). CERR (pronounced "sir") is an open source, freely available, general treatment plan analysis package written in Matlab (high-level data analysis, programming, and visualization package from Mathworks, Inc; http:\\www.mathworks.com). CERR capabilities for radiotherapy treatment response modeling include the following: (1) ability to import full treatment planning data sets (including CT scans, structure sets, dose distributions, DVHs, beam geometries) from a wide range of clinical and commercial treatment planning systems; (2) convenient graphical review which is crucial for verification of data manipulation correctness; (3) contouring; (4) programmable access to the data with human-readable, meta data objects; and (5) ability to register images using rigid and deformable tools, etc. A snapshot of CERR viewer, navigation montage and contouring tool are shown in Figure 1.

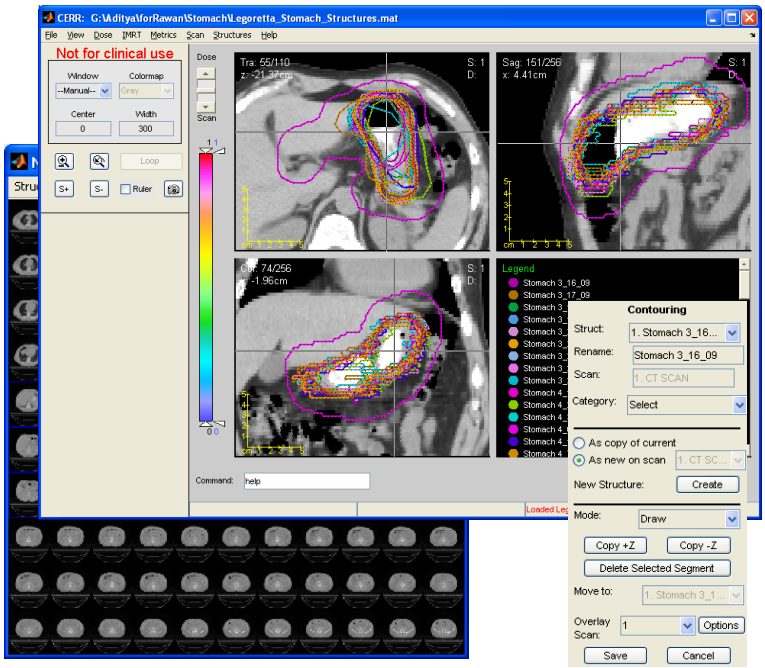

Figure 1. A snapshot from the CERR user interface.

2.1 Union structure from daily images in CERR

The treatment planning scans and daily images along with structures could be imported in CERR from the DICOM or the RTOG format. After registering the images, structures are copied to a reference scan (e.g., the treatment plan). An alternative approach is to use commercial software such as Pinnacle to register and copy the contours, then import the resulting RT structure object into CERR for further manipulation.

2.2 Estimation of the organ motion probability

The union of the original structures (without margin included) from daily images is created to encompass the entire tumor region. We would like the structure created by expanding the planning structure by the suggested margin to match closely with this union structure. If the structures from all the daily images are included within the expanded structure, then 100% of tumor would be treated. But, this would also lead to normal tissue being irradiated excessively. Hence, we

*elnaqa@wustl.edu; phone +1 314 362 0129; fax +1 314 362 8521; radonc.wustl.edu

doi: 10.5166/jroi-2-1-7

ISSN: 1663-618X, J Radiat Oncol Inform 2010; 2:1:9-19

define a confidence level (ℓ) so that the planning structure when expanded with the suggested margin would cover at least ℓ % of the tumor images union. This can also be thought of as ℓ % probability that an organ is present at any given location. Any confidence level less than 100% would lead to smaller margins and spare normal tissue. Once the union structure with ℓ % confidence is created by combining the information from all the available daily images as discussed below, the optimization problem is set-up in order to compute optimal anisotropic margins which, when added to the planning structure, would lead to a structure similar to the union structure with ℓ % confidence.

3. ESTIMATION OF OPTIMAL MARGINS

3.1 Overview

Figure 2 shows the basic steps of using the software tool to perform image margin estimation. After a set of images is imported, rigid image registration is applied to align all the images.

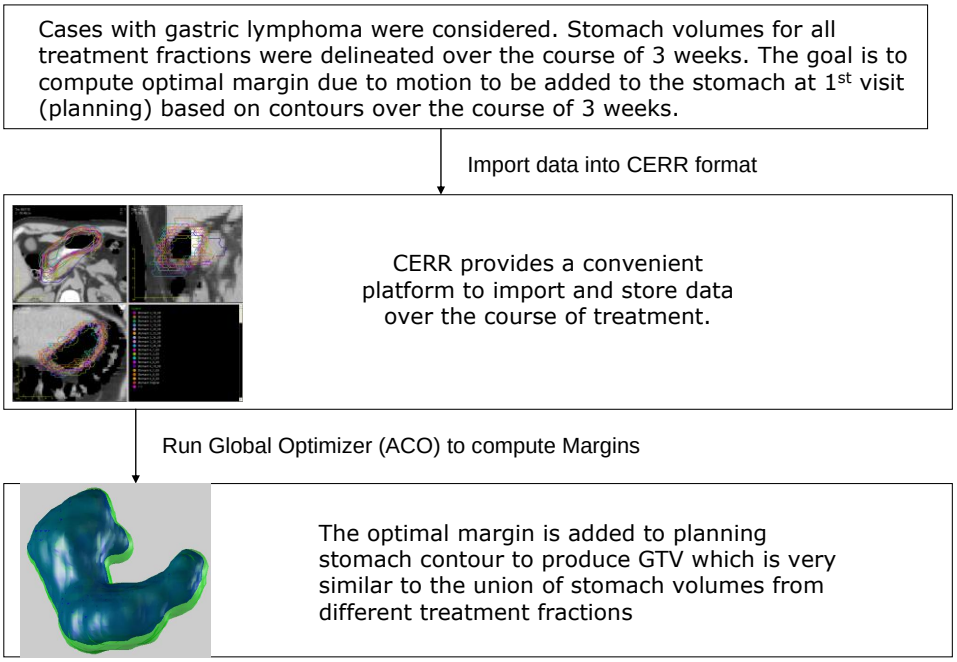

Figure 2. The main workflow of the ACO algorithm for margin estimation.

3.2 Anisotropic Expansion of Structure

In order to expand the stomach anisotropically, all the points within the stomach were convolved with an ellipsoid. The ellipsoid convolute is represented by Eq. (1).

$$\left(\frac{x-x_c}{\sigma_x}\right)^2+\left(\frac{y-y_c}{\sigma_y}\right)^2+\left(\frac{z-z_c}{\sigma_z}\right)^2 \le 1 \qquad (1)$$

(x_c , y_c , z_c) are the coordinates of the center of the ellipsoid and (σ_x, σ_y, σ_z) are the lengths of axes along x, y and z directions.

*elnaqa@wustl.edu; phone +1 314 362 0129; fax +1 314 362 8521; radonc.wustl.edu

doi: 10.5166/jroi-2-1-7

ISSN: 1663-618X, J Radiat Oncol Inform 2010; 2:1:9-19

Notice that Eq. (1) reduces to an equation of a sphere if all the axes are of equal length. Here we are interested in having different margins along (+)ve and (-)ve directions with respect to the iso-center. In order to achieve this, we shift the center of ellipsoid such that the margins along (+)ve and (-)ve directions are as specified. For example, if we want to add a margin of σ_{-x} and σ_{+x} along (-)ve and (+)ve x-directions respectively, then the axis length σ_x would be computed as $\sigma_{-x} + \sigma_{+x}$ and the centroidal coordinate would be ($\sigma_{-x} + \sigma_{+x}$)/2. The same would be true for remaining axes as well. The anisotropic expansion was tested and verified on basic geometric shapes. Figure 3 shows an anisotropically expanded cubical object using the above procedure.

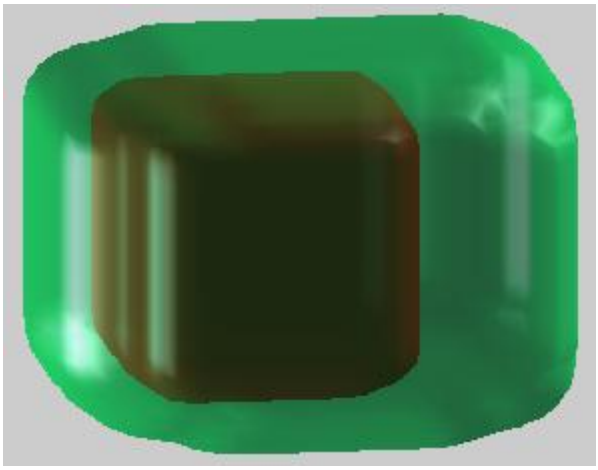

Figure 3. An approximate cubical object is expanded by margins of 1 cm in all directions except one.

3.3. Problem Formulation and Optimization Algorithm

The goal is to compute optimal margins along (-)ve and (+)ve x, y and z directions in order to maximize similarity (dice metric) between the union of stomach contours over all treatment fractions for the specified confidence level and the structure expanded with suggested margins. The margins are equivalent to the lengths of convolute ellipsoid axes. The problem statement is as follows.

Compute: $\sigma_{-x}, \sigma_{+x}, \sigma_{-y}, \sigma_{+y}, \sigma_{-z}, \sigma_{+z}$

To Maximize: $2 \times \dfrac{volume\left(A \cap B\right)}{volume\left(A\right) + volume\left(B\right)}$ (2)

Subject to: Bound constraints $0 \leq \sigma_{-x}, \sigma_{+x}, \sigma_{-y}, \sigma_{+y}, \sigma_{-z}, \sigma_{+z} \leq 3$ cm

where

σ_{-x} is the margin in (-)ve x direction (i.e. the length of convolute ellipsoid in (-)ve x direction),

σ_{+x} is the margin in (+)ve x direction (i.e. the length of convolute ellipsoid in (+)ve x direction) and so on,

A refers to the union of stomachs over all treatment fractions,

B refers to the structure created by adding anisotropic margins.

*elnaqa@wustl.edu; phone +1 314 362 0129; fax +1 314 362 8521; radonc.wustl.edu

doi: 10.5166/jroi-2-1-7

 ISSN: 1663-618X, J Radiat Oncol Inform 2010; 2:1:9-19

Since the objective function (Dice metric (Eq. 2)) is highly nonlinear, a gradient based optimizer would get stuck in local solution. In this work, we used a global optimizer based on the prey catching strategy of ants (Monmarche, Venturini and Slimane, 2000). The next section gives a brief description of ant colony optimization algorithm used in this work.

3.4. Ant Colony Optimization

In the last decade various algorithms have been researched to solve optimization problems based on the prey catching behavior of ants. Such algorithms find applications in robotics, objects clustering, communication network and combinatorial optimization. The ants whose behavior was modeled in this work are found in the Mexican desert and are known as Pachycondyla apicalis (Monmarche, Venturini and Slimane, 2000). These ants use visual cues as a feedback mechanism for catching prey. They use simple principles to search for their prey, both from global and local viewpoints. Starting from their nest, they globally cover a given surface by partitioning it into many hunting sites. Each ant performs a local random exploration of its hunting sites and the choice of site is sensitive to the success previously met on this site. These principles have been translated into an algorithm to obtain global optimal solutions of unconstrained and constrained optimization problems (Monmarche, Venturini and Slimane, 2000, Apte and Wang, 2004). Following is a brief algorithm based on the behavior of these ants.

Table 1. Ant Colony Optimization

(1) **Choose** randomly the initial nest location ***N***. This is the starting point to the algorithm.
(2) For each ant a_i, $i \in [1 \ldots n]$:
If a_i has less than *p* hunting sites in memory, then **Create** a new site in the neighborhood of ***N*** and explore the created site
Else
If the previous site exploration was successful then **Explore** again the same site
Else **Explore** a randomly selected site (among the *p* sites in memory)
(3) Remove from the ants memories all sites which have been explored unsuccessfully more than $P_{local}(a_i)$ consecutive times.
(4) Perform recruitment (best site copying between two randomly selected ants)
(5) If more than *T* iterations have been performed Then **Change** the nest location and **Reset** memories of all ants
(6) Go to (2) or Stop if a stopping criteria is satisfied

Figure 4 illustrates the global and local hunting strategy. The parameters which govern the spread of global and local sites are Asite and Alocal. Based on the actual behavior of ants these parameters are set such that Asite/Alocal = 10. Figure 5 illustrates the convergence of the algorithm by moving the nest to more interesting areas of the design space. Readers are encouraged to refer to (Monmarche, Venturini and Slimane, 2000) for in depth information about the recruitment process and the performance of the algorithm.

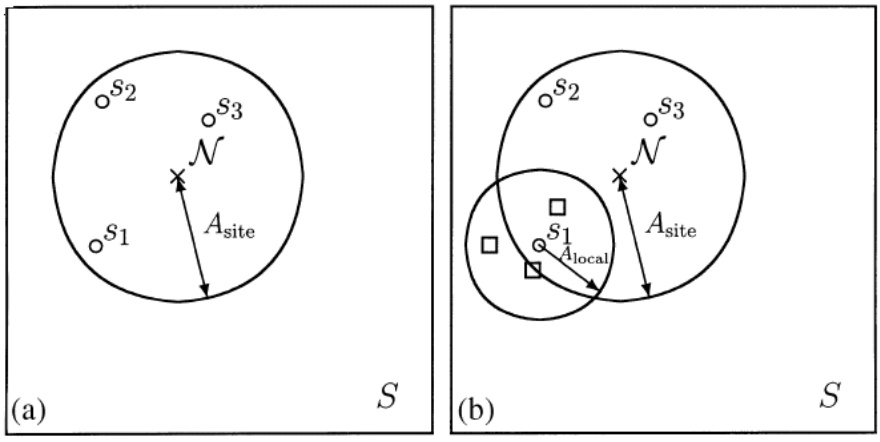

*elnaqa@wustl.edu; phone +1 314 362 0129; fax +1 314 362 8521; radonc.wustl.edu

doi: 10.5166/jroi-2-1-7
 ISSN: 1663-618X, J Radiat Oncol Inform 2010; 2:1:9-19

Figure 4. Illustration of Global and Local search mechanism: (a)The sites *s*1, *s*2 and *s*3 are randomly generated and their assigned maximum distance from the nest ***N*** is given as *A*site, (b) The squares represent the local explorations of site *s*1 at a maximum distance *Alocal* from *s*1. (From (Monmarche, Venturini and Slimane, 2000) with permission).

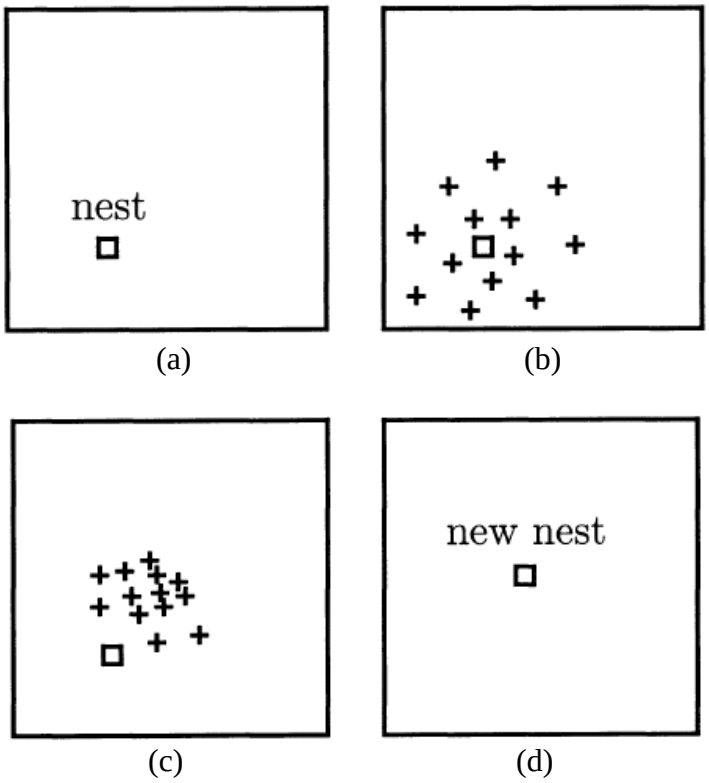

Figure 5. Illustration of the Ant algorithm. In (a), the nest is randomly selected in the search space. Then, in (b), hunting sites are randomly created around the nest according to the distribution generated by the Asite parameters. In (c), due to the local explorations, hunting sites move towards more interesting areas of the search space (here the center of the space in our example). Then, in (d), the nest moves to the best generated point so far. Hunting sites are then created again as in (b), and so on. (From (Monmarche, Venturini and Slimane, 2000) with permission).

4. EXAMPLE APPLICATIONS AND RESULTS

4.1. Dataset

As a demonstrative example we considered a case of a gastric lymphoma patient who was treated on a TomoTherapy machine and received daily megavoltage CT imaging (MVCT). The gastric volume was controlled for simulation (daily imaging) with a 6 hour fast and administration of 80 or 100 cc of contrast (water) prior to treatment. The stomach volumes were identified and contoured on each daily MVCT scan by two observers (MJ and DM). The presented results are intended for demonstration purposes of the proposed methodology and should not be considered as clinical findings, which will be presented elsewhere.

*elnaqa@wustl.edu; phone +1 314 362 0129; fax +1 314 362 8521; radonc.wustl.edu

doi: 10.5166/jroi-2-1-7
 ISSN: 1663-618X, J Radiat Oncol Inform 2010; 2:1:9-19

4.2. Stomach motion probability

An example showing the estimation of motion probability is given in Figure 6. It is noted that as the margin is increased, the coverage of stomach over treatment fraction increases and so does the excessively irradiated regions. This plot can be used as a guidance to generate a GTV volume. It can be inferred from this plot that a margin of 1.5cm to the original stomach volume would achieve reasonable coverage and result in 500cc being irradiated in excess. Note that setup errors are ignored in this case; however, they could be included in each daily image case and integrated into the margin effect estimate.

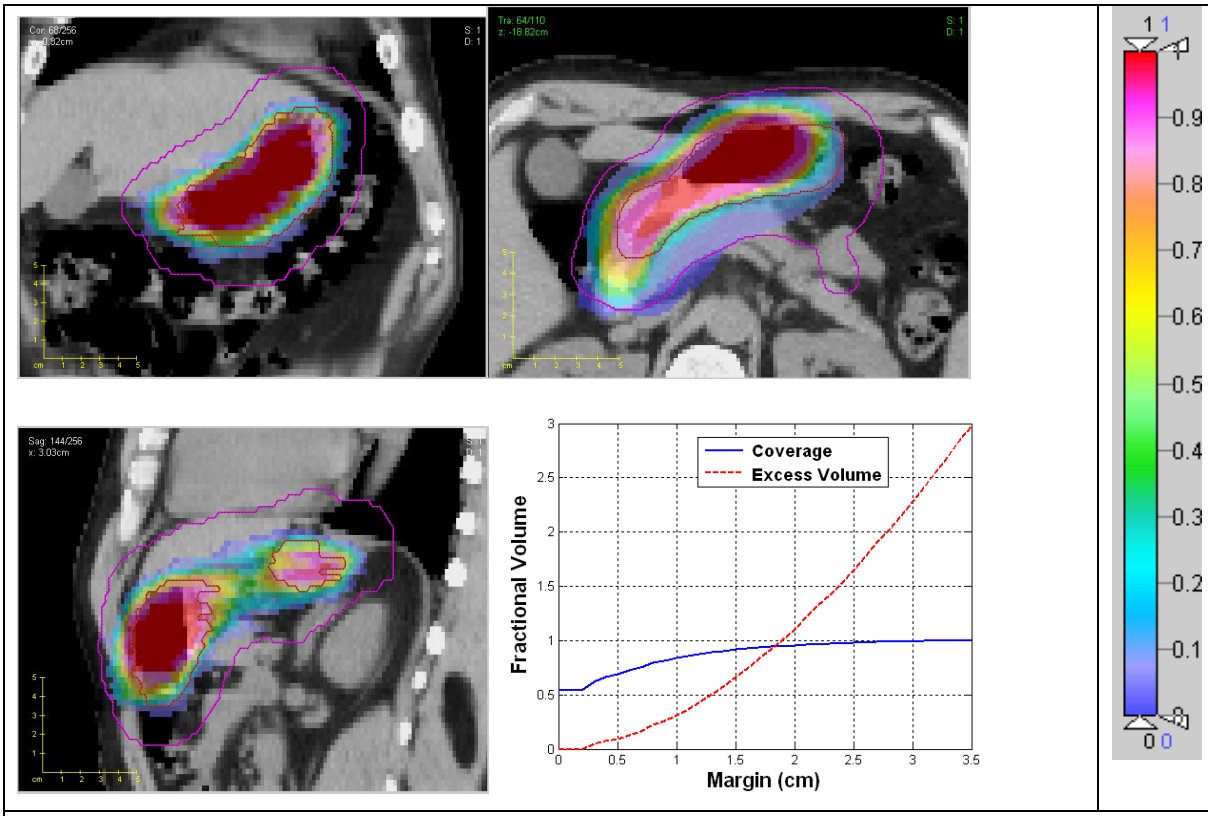

Figure 6. (i) Top Left: Transverse view, (ii) Top Right: Sagittal view, (iii) Bottom Left: Coronal view of the CT scan. The outer contour is the GTV used for treatment planning. The inner contour represents the original stomach volume. The colorwash represents overlaps between stomach volumes over the course of treatment; red being the highest and blue being the lowest overlap. As observed, there is quite a bit of volume which receives excess irradiation. (iv) Bottom Right: Volume versus Margin added to the original stomach volume.

4.3. Optimal margin estimation

Optimal margins for 75% and 95% coverage of the stomach were computed for the same patient. The problem formulation and optimization algorithm outlined in section 3 were used. A total of 12500 function evaluations were performed to reach the optimal solution. Note that these many function evaluations are just a fraction of what would be required for a simple grid search. For example, if we consider a grid with a resolution of 0.2 cm within a range of 0 to 3 cm, then we would require 4.7018e+011 function evaluations to search the entire 6-dimensional grid.

Margin for 75% coverage

*elnaqa@wustl.edu; phone +1 314 362 0129; fax +1 314 362 8521; radonc.wustl.edu

doi: 10.5166/jroi-2-1-7

 ISSN: 1663-618X, J Radiat Oncol Inform 2010; 2:1:9-19

In Figure 7, we show the ACO progression for estimating 75% probability of stomach motion coverage. The estimated optimal margins are:

$(x_n, x_p, y_n, y_p, z_n, z_p)$ = (0.4107, 0.0027, 0.1205, 1.0319, 0.1561, 0.3197) cm

Figure 8 shows 2-D and 3-D views of the original and expanded stomach structure.

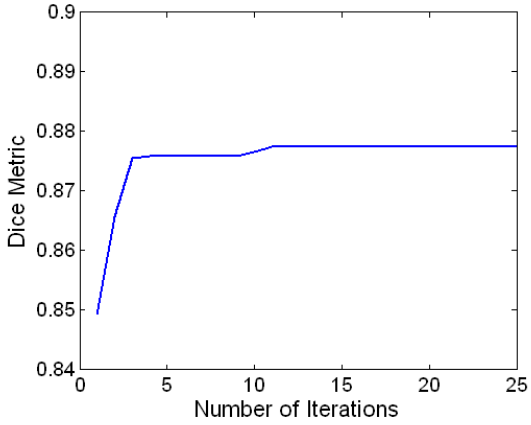

Figure 7. Optimization History for 75% coverage. ACO was run for 25 nest relocations. The algorithm converged in about 10 iterations with an optimal dice metric of 0.8774

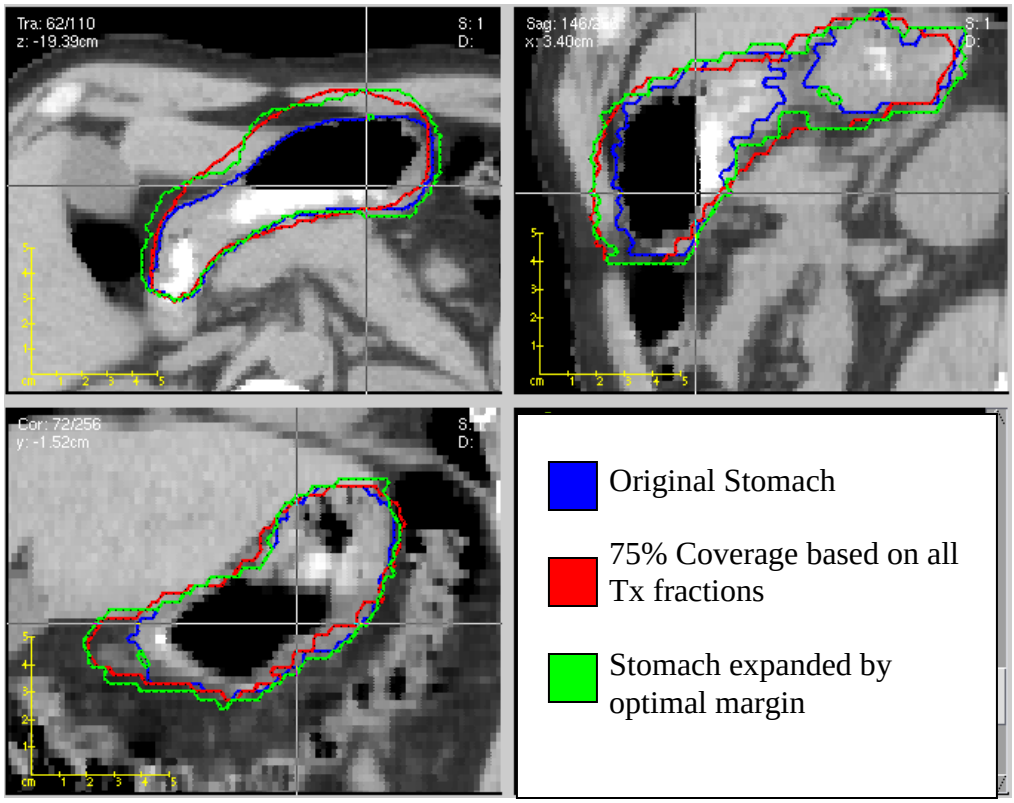

*elnaqa@wustl.edu; phone +1 314 362 0129; fax +1 314 362 8521; radonc.wustl.edu

doi: 10.5166/jroi-2-1-7

ISSN: 1663-618X, J Radiat Oncol Inform 2010; 2:1:9-19

(a)

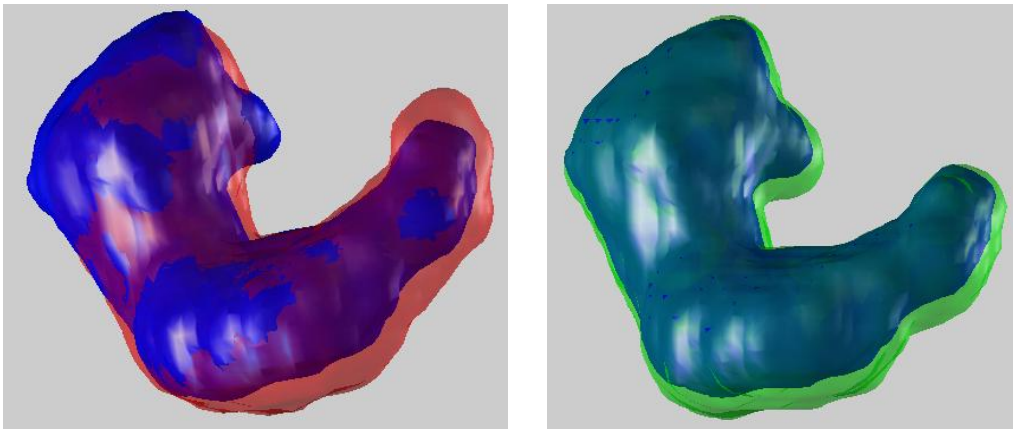

(b) (c)

Figure 8. (a) Transverse, sagittal and coronal views of original stomach, 75% coverage over all Tx fractions and stomach expanded by the optimal margin. (b) 3-d view of original stomach and 75% coverage. (red) (c) 3-d view of original stomach and stomach with optimal margin (green).

Margin for 95% coverage

In Figure 9, we show the ACO progression for estimating 95% probability of stomach motion coverage. The estimated optimal margins are:

$(x_n, x_p, y_n, y_p, z_n, z_p)$= (0.9215, 0.3209, 0.5826, 1.4086, 0.1389, 0.6693) cm

Figure 10 shows 2-D and 3-D views of the original and expanded stomach structure.

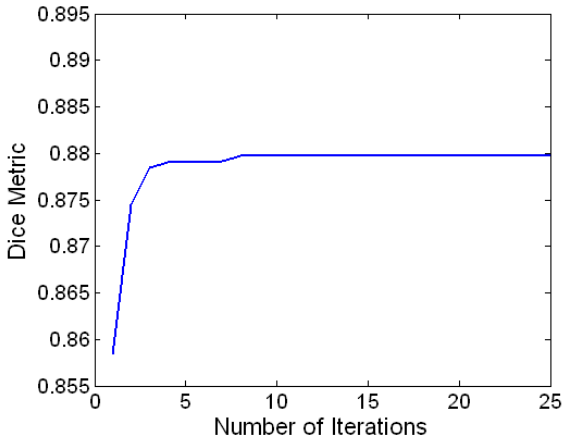

*elnaqa@wustl.edu; phone +1 314 362 0129; fax +1 314 362 8521; radonc.wustl.edu

doi: 10.5166/jroi-2-1-7

 ISSN: 1663-618X, J Radiat Oncol Inform 2010; 2:1:9-19

Figure 9. Optimization History for 95% coverage. ACO was run for 25 nest relocations. The algorithm converged in about 10 iterations with an optimal dice metric of 0.8797.

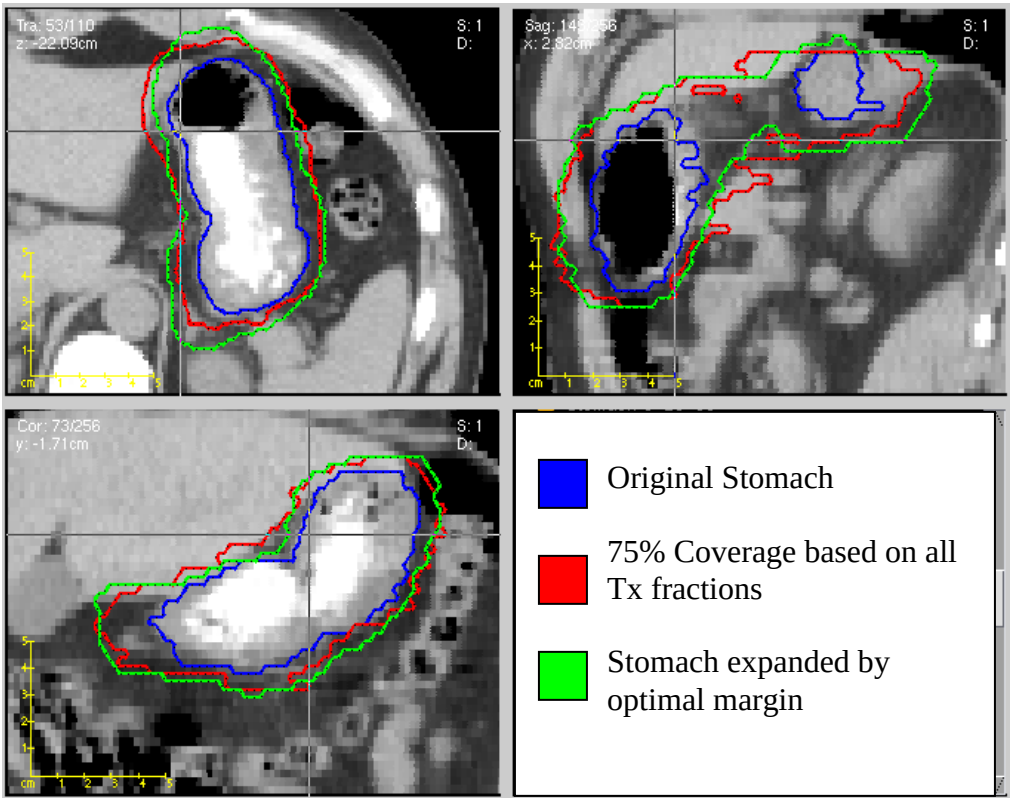

(a)

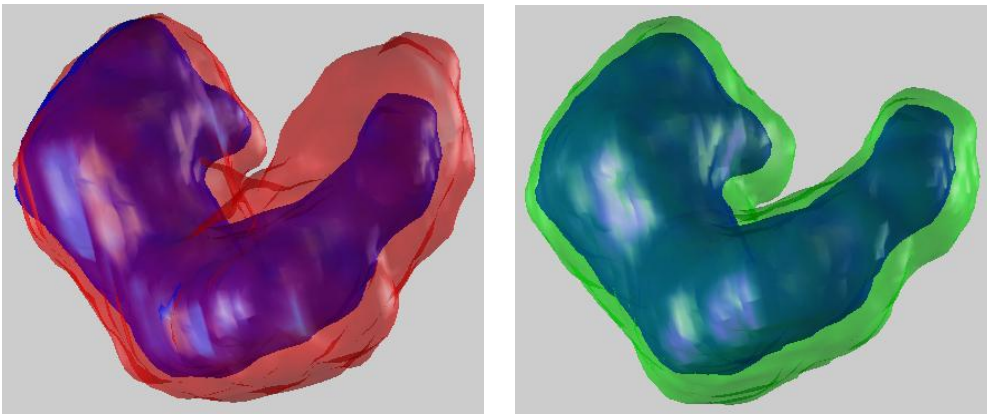

(b) (c)

Figure 10. (a) Transverse, sagittal and coronal views of original stomach, 95% coverage over all Tx fractions and stomach expanded by optimal margin. (b) 3-d view of original stomach and 95% coverage. (c) 3-d view of original stomach and stomach with optimal margin.

*elnaqa@wustl.edu; phone +1 314 362 0129; fax +1 314 362 8521; radonc.wustl.edu

doi: 10.5166/jroi-2-1-7

ISSN: 1663-618X, J Radiat Oncol Inform 2010; 2:1:9-19

5. DISCUSSION AND CONCLUSIONS

In this work, we have presented a new software tool and an algorithm for estimating organ motion margins from daily images, which could be used to derive more accurate planning target volumes (PTVs). Clinically, errors due to patient-setup would be combined with motion errors estimated by the software tool to achieve such accuracy without compromising tumor coverage or over-dosing surrounding normal tissue. The process consists of two main steps that involve deriving organ motion probability and estimating the optimal margin. For motion probability, we used methods based on rigid registration available with CERR. However, more accurate estimates could be obtained by utilizing deformable registration algorithms (Yang, Lu, Low, Deasy, Hope and El Naqa, 2008). The estimation of the optimal margin was carried out using swarm intelligence based on the ACO algorithm. These algorithms can provide efficient estimates of the optimal margin extent in each direction compared to an exhaustive search while achieving a global optimal solution as demonstrated in our results in gastric lymphoma. Furthermore, our results indicate that the developed tool can provide improved visualization and quantification of daily deformations for estimating isotropic and anisotropic margins for radiotherapy treatment plans in cases where organ motion is an issue such as the presented example of gastric lymphoma, or in cases of lung and prostate cancers.

6. REFERENCES

[1] Webb, S. Contemporary IMRT : developing physics and clinical implementation. Bristol ; Philadelphia: Institute of Physics. 2005.

[2] Van Herk, M. Errors and margins in radiotherapy. Semin Radiat Oncol 2004;14:52-64.

[3] Deasy, JO, Blanco, AI, Clark, VH. CERR: A Computational Environment for Radiotherapy Research. Medical physics 2003;30:979-985.

[4] Monmarche, N, Venturini, G, Slimane, M. On how Pachycondyla apicalis ants suggest a new search algorithm. Future Generation Computer Systems 2000;16:937-946.

[5] Apte, A, Wang, BP. Using power of Ants for Optimization. 45th AIAA/ ASME/ ASCE/ AHS/ ASC Structures, Structural Dynamics and Materials Conference, Palm Springs, California: AIAA. 2004.

[6] Yang, D, Lu, W, Low, DA, Deasy, JO, Hope, AJ, El Naqa, I. 4D-CT motion estimation using deformable image registration and 5D respiratory motion modeling. Med Phys 2008;35:4577-4590.

*elnaqa@wustl.edu; phone +1 314 362 0129; fax +1 314 362 8521; radonc.wustl.edu

doi: 10.5166/jroi-2-1-7

 ISSN: 1663-618X, J Radiat Oncol Inform 2010; 2:1:9-19